

OPEN

The Role of Parvalbumin-positive Interneurons in Auditory Steady-State Response Deficits in Schizophrenia

Christoph Metzner^{1,3*}, Bartosz Zurowski² & Volker Steuber³

Despite an increasing body of evidence demonstrating subcellular alterations in parvalbumin-positive (PV⁺) interneurons in schizophrenia, their functional consequences remain elusive. Since PV⁺ interneurons are involved in the generation of fast cortical rhythms, these changes have been hypothesized to contribute to well-established alterations of beta and gamma range oscillations in patients suffering from schizophrenia. However, the precise role of these alterations and the role of different subtypes of PV⁺ interneurons is still unclear. Here we used a computational model of auditory steady-state response (ASSR) deficits in schizophrenia. We investigated the differential effects of decelerated synaptic dynamics, caused by subcellular alterations at two subtypes of PV⁺ interneurons: basket cells and chandelier cells. Our simulations suggest that subcellular alterations at basket cell synapses rather than chandelier cell synapses are the main contributor to these deficits. Particularly, basket cells might serve as target for innovative therapeutic interventions aiming at reversing the oscillatory deficits.

Since synchronized neuronal activity is thought to underlie efficient communication in the brain^{1–3} and to be crucially involved in working memory processes⁴, alterations of this synchrony, as found in electroencephalogram (EEG) or magnetoencephalogram (MEG) studies of patients suffering from schizophrenia (SCZ)^{5,6}, might contribute to the symptoms in patients and impairments characterizing schizophrenia. One very robust finding in EEG/MEG studies of schizophrenia patients is a deficit in the gamma band auditory steady state response (ASSR)^{7–17}.

Fast-spiking (FS), PV⁺, γ -amino-butyric acidergic (GABAergic) interneurons seem to be a major contributor to gamma oscillations^{18,19}. However, this class of inhibitory interneurons can be further divided into at least two subgroups: basket cells (BCs) and chandelier cells (ChCs)^{20,21}. The main difference between basket and chandelier cells is their axonal target. While basket cells mainly target the perisomatic region of excitatory pyramidal cells and other inhibitory interneurons, chandelier cells exclusively target the axon hillock of pyramidal cells (PCs)²⁰. Furthermore, although their electrophysiological properties are similar subtle differences, such as different afterhyperpolarization amplitudes and firing frequencies, between the two subclasses exist²². Lastly, while BC synapses display fast and strong inhibition, ChC synapses have been shown to have a depolarizing effect *in vitro*^{23–26}. However, whether this depolarization also exists *in vivo* and whether it has an excitatory or rather a predominantly shunting effect remains elusive. Moreover, it is not clear so far whether these differences also imply a different involvement in the generation of gamma oscillations.

Several alterations of PV⁺ neurons have been found in schizophrenia. While the density of PV⁺ neurons does not seem to be altered in subjects with schizophrenia^{27,28}, the levels of mRNA for the calcium-binding protein PV are markedly reduced²⁹. Furthermore, 50% of PV⁺ neurons in dorsolateral prefrontal cortex lack detectable levels of the 67 kDa isoform of glutamate decarboxylase (GAD₆₇), an enzyme that catalyzes the decarboxylation of glutamate to GABA²⁹. It has been suggested that the reduced expression of GAD67 mRNA, the gene encoding the GAD₆₇ enzyme, likely implies a reduction in GABA synthesis in cortical GABA neurons, which in turn would

¹Neural Information Processing Group, Institute of Software Engineering and Theoretical Computer Science, Technische Universität Berlin, Berlin, 10623, Germany. ²Center for Integrative Psychiatry, University of Lübeck, Lübeck, 23562, Germany. ³Biocomputation Group, Centre for Computer Science and Informatics Research, University of Hertfordshire, Hatfield, AL10 9AB, United Kingdom. *email: cmetzner@ni.tu-berlin.de

lead to smaller amplitude IPSCs at the postsynaptic site³⁰. Furthermore, a reduction in the plasma membrane GABA transporter GAT1, which is a major contributor to the specificity of synapses by preventing spillover to neighbouring synapses^{31,32}, has been found in PV⁺ interneurons in patients with schizophrenia²⁷. A reduction in GAT1 leads to a prolongation of IPSC durations^{31,32}. Interestingly, in patients with schizophrenia, immunoreactivity for the GABA-A α_2 subunit is increased³³ in the axon initial segment of pyramidal cells, the exclusive target of chandelier cell cartridges. GABA receptors with an α_2 subunit, compared to receptors with an α_1 subunit, also show an increase in IPSC duration in transfected human embryonic cells³⁴. In summary, the reduced expression of GAD67, the reduction of GAT1 and increased α_2 subunit expression in SCZ patients have two main effects: a reduction of inhibitory strength of PV⁺ neurons (both BCs and ChCs) and an increased IPSC duration at PV⁺ synapses (also for both BCs and ChCs, however, considerably longer for ChCs). These cellular differences in PV⁺ neurons are likely to have an influence on oscillatory activity. Since gamma oscillation generation and maintenance crucially depends on fast-spiking PV⁺ interneurons, changes in peak amplitude and duration of IPSCs might particularly affect oscillations in this frequency band.

In addition to evidence suggesting an immediately compromised GABAergic system, the finding that N-methyl-D-aspartate receptor (NMDAR) antagonists (such as phencyclidine and ketamine) produce symptoms very similar to key clinical features of schizophrenia³⁵, sparked the idea that the underlying cause of the disturbance of the GABAergic circuitry might be a secondary effect of an NMDAR hypofunction at GABAergic interneurons. While studies exploring the idea that the hypofunction was due to less receptors have produced mixed results³⁶, convergent lines of evidence underpin the hypothesis that NMDARs are dysfunctional in schizophrenia patients³⁷. Direct evidence in favour of this hypothesis are for example, changes in NMDAR-associated protein levels at the postsynaptic site³⁸, a reduction in NMDAR-mediated signalling following neuregulin 1 activation of ErbB4 receptors³⁹, lower levels of glutathione (a modulator at the redox-sensitive site of NMDARs)⁴⁰ and a reduction of kynurenine 3-monooxygenase which might increase kynurenic acid (an NMDAR antagonist) levels⁴¹.

Earlier modelling efforts by Vierling-Claassen *et al.*^{8,42}, proposed that increased IPSC decay times at chandelier cell synapses might be sufficient to explain the gamma and beta range ASSR deficits in schizophrenia patients. However, while demonstrating that, in principle, increased IPSC decay times at chandelier cell synapses could result in experimentally observed ASSR deficits for patients with SCZ, Vierling-Claassen *et al.* did not consider the relatively small number of chandelier cells compared to basket cells⁴³. Furthermore, they did not take into account potentially increased IPSC decay times at basket cell synapses, changes in excitability of interneurons due to NMDAR hypofunction and the putative excitatory effect of ChC-mediated neurotransmission. Therefore, we extended their computational model to investigate the differential role of prolonged IPSC decay time at basket and chandelier cell synapses, at realistic ratios of chandelier to basket cells, in gamma and beta range ASSRs. We found that, while prolonged IPSC decay times at chandelier cells could explain experimental results when chandelier cells form 50% of inhibitory neurons in the network, they failed to do so at lower, more realistic percentages such as 10% or even 5%. In contrast, for physiologically plausible chandelier cell percentages of 10% or 5%, prolonged IPSC decay times at basket cell synapses were able to reproduce experimental findings. Increased IPSC decay times at synapses of both interneuron subtypes resulted in qualitatively very similar ASSRs as for changes at basket cell synapses only, suggesting that chandelier cell alterations might not be crucially involved in gamma and beta range ASSR deficits in schizophrenia. We then wondered whether a potentially excitatory effect of chandelier cells onto pyramidal cells could explain the deficits but found that, at low chandelier cell percentages, it had a negligible effect on the overall network in general and on gamma and beta range ASSRs specifically. Lastly, decreased excitability of chandelier cells at low chandelier cell percentages, as a consequence of reduced, tonic NMDAergic excitation, did not produce ASSR deficits consistent with experimental observations, in fact, it hardly changed the network behaviour at all.

Results

In order to explore the roles chandelier and basket cells play in the emergence of oscillatory entrainment deficits in schizophrenia patients, we simulated the effects of cellular and molecular abnormalities of both cell types found in schizophrenia, focusing on GABAergic synapses. We started with an investigation of abnormalities of chandelier cells in isolation, followed by abnormalities of basket cells in isolation and an exploration of interactions of abnormalities in both cell types, followed by an exploration of the potentially excitatory ChC-PC coupling. We concluded with an exploration of NMDAR hypofunction at ChC interneurons and its interplay which changes at GABAergic synapses in determining the oscillatory behaviour of the network.

We simulated the effect of GABAergic abnormalities for four different conditions with a BC/ChC ratio of 50%, 25%, 10% and 5%, respectively. As results at high ChC percentages (50 and 25%) were similar and results at low ChC percentages (10 and 5%) were also similar, we only present results for 50% and 10%. Based on the investigation of the GABAergic alterations, we focused on low ChC percentages of 10% when exploring the excitatory ChC-PC coupling and the NMDAR hypofunction.

Alterations of chandelier cells. As explained earlier, the plasma membrane GABA transporter GAT1 is reduced in chandelier cell synapses onto the axon initial segment of cortical pyramidal neurons, resulting in a prolongation of IPSC decay times. Additionally, the α subunit composition of the GABA_A receptors at the axon initial segment is skewed towards the α_2 subunit in comparison to receptors at the dendrites, which leads to an even more prominent prolongation of decay times. This increased time course of inhibition at chandelier cell synapses has been proposed to account for the characteristic oscillatory entrainment changes in the gamma and beta range by Vierling-Claassen *et al.*^{8,42}. However, in their studies two important aspects of the local microcircuitry have not been accounted for: 1) the relatively small number of chandelier cells (compared to basket cells)⁴³ and 2) the specific connectivity scheme of chandelier cells, i.e. the fact that chandelier cells do not form

Exp. study	Measure				
	40/40	30/30	20/20	40/20	20/40
Kwon <i>et al.</i> ⁷	↓	—	—	—	—
Vierling-Claassen <i>et al.</i> ⁸	↓	—	↑	↓	↑
Krishnan <i>et al.</i> ⁹	↓	—	—	—	—

Table 1. Summary of ASSR deficits in patients with schizophrenia in the three studies considered here (↓: significantly lower in patients, ↑: significantly higher in patients, —: no significant difference between controls and patients).

connections with themselves⁴⁴. We explored whether prolonged IPSC decay times at chandelier cell synapses ($\tau_{ChC} = 28$ ms, as in Vierling-Claassen *et al.*⁸) could still explain schizophrenia-like entrainment deficits when these two aspects were included in the model.

At a ChC percentage of 50, the 40/40 measure was drastically reduced in the ‘schizophrenia-like’ network, reflecting a disturbance in the generation of gamma oscillations, which is in line with experimental evidence (see Table 1). However, the other entrainment measures did not match with experimental findings. The 30/30 measure was also strongly reduced, meaning that the disturbance in the generation of oscillations was not restricted to the gamma range at around 40 Hz. Furthermore, the 20/20 measure did not differ strongly between the ‘schizophrenia-like’ and the control network, while a difference was found in experimental studies (see Thune *et al.*¹⁷). Lastly, the emergence of a large 20/40 measure, which has been observed in the experimental study of Vierling-Claassen *et al.* as well as in their modelling work⁸, could not be seen. As can be seen in Fig. 1, the 20/40 measure, although higher than in the control network, remained small (note the scale in the 20/40 plot of Fig. 1(b)).

At lower, more realistic, values of ChC percentage hardly any difference of the MEG signals and the five entrainment measures between control and ‘schizophrenia-like’ networks could be seen (see Fig. 1). Note that this did not change with further increases of the IPSC decay times (we tested $\tau_{ChC} = 35$ ms and $\tau_{ChC} = 40$ ms; data not shown). This suggests that prolonged IPSC decay times at ChC synapses are not sufficient to induce schizophrenia-like alterations in oscillatory entrainment.

Alterations of basket cells. The plasma membrane GABA transporter GAT1 is also reduced in basket cell synapses onto dendrites in the perisomatic region of cortical pyramidal neurons, again resulting in a prolongation of IPSC decay times at these synapses²⁷. However, opposed to chandelier cells, GABA_A receptors at basket cell synapses predominantly contain the α_1 subunit³³. This means that the IPSC decay time increases at BC-PC synapses probably also exist in schizophrenia patients but the increase is likely to be smaller than that at the ChC-PC synapses we examined before. Therefore, we initially chose an increased IPSC decay time of $\tau_{BC} = 20$ ms.

At high ChC percentages, this alterations had hardly any effect on the oscillatory behaviour of the network in response to any of the three driving frequencies tested (see Fig. 2(a) top row and Fig. 2(b)).

At low, more realistic ChC percentages this alteration led to changes of oscillatory entrainment more in line with experimental evidence (see Fig. 2). Specifically, the gamma range entrainment was significantly disturbed, reflected by the strong decrease of the 40/40 measure. Furthermore, a characteristic increase of the 20/20 measure was also clearly visible. The changes were restricted to the gamma and beta band leaving the respective border intact, i.e. the 30/30 measure was not significantly altered. However, the emergence of a strong 20/40 measure, seen by Vierling-Claassen *et al.*⁸, both in experiment and model, was not visible. Figure 2(b) (middle panel) does show an increase of the 20/40 measure compared to control, however it remains small.

Therefore, we increased the IPSC decay time at BC-PC synapses further to $\tau_{BC} = 28$ ms. For high ChC percentages, the further increase of τ_{BC} led to a strong decrease of the 40/40 measure but only had minor effects on all other entrainment measures (lower row of (a) and the third panel of (b) of Fig. 3).

As shown in Fig. 3 (lower row of (a) and the third panel of (b)), in the case of low ChC percentages, this led to a prominent increase of the 20/40 measure, similar to what was found in experiments⁸. Figure 4(a) shows the evolution of this 20 Hz peak for 40 Hz drive over three different values of $\tau_{BC} = 20$ ms (black), 24 ms (red) and 28 ms (green). While the PCs are still able to recover from inhibition within every gamma cycle for $\tau_{BC} = 20$ ms, for larger values of τ_{BC} , more and more PCs are suppressed during every other gamma cycle, giving rise to a prominent 20 Hz peak. Interestingly, however, the longer IPSC decay time of $\tau_{BC} = 28$ ms did not only effect the 20/40 measure but also led to a strong decrease of the 30/30 measure, which then became markedly different from the 30/30 measure of the control network (see Figs. 3 and 4(b)). This is in disagreement with experimental findings.

Alterations of chandelier and basket cells. The results presented in the previous sections suggest that ChCs (at realistic numbers) are unable to produce ‘schizophrenia-like’ gamma and beta entrainment deficits in isolation and that BCs are the major contributor to these. However, alterations at ChCs might nevertheless modulate the deficits produced by BC alterations. Therefore, we next looked at the interactions of simultaneous alterations at BCs and ChCs.

First, we simulated the combined effect of a moderate increase of IPSC decay times at both ChC-PC and BC-PC synapses, with a stronger increase at ChC-PC synapses (i.e. $\tau_{ChC} = 28$ ms and $\tau_{BC} = 20$ ms).

Here, for high ChC percentages, we found a strong decrease of the 40/40 and the 40/20 measures (Fig. 5), in line with experimental evidence of a gamma deficit in schizophrenia^{7,8,17}. Furthermore, the 20/40 measure was increased, although still low. However, both the 20/20 and the 30/30 measure were also strongly reduced in this

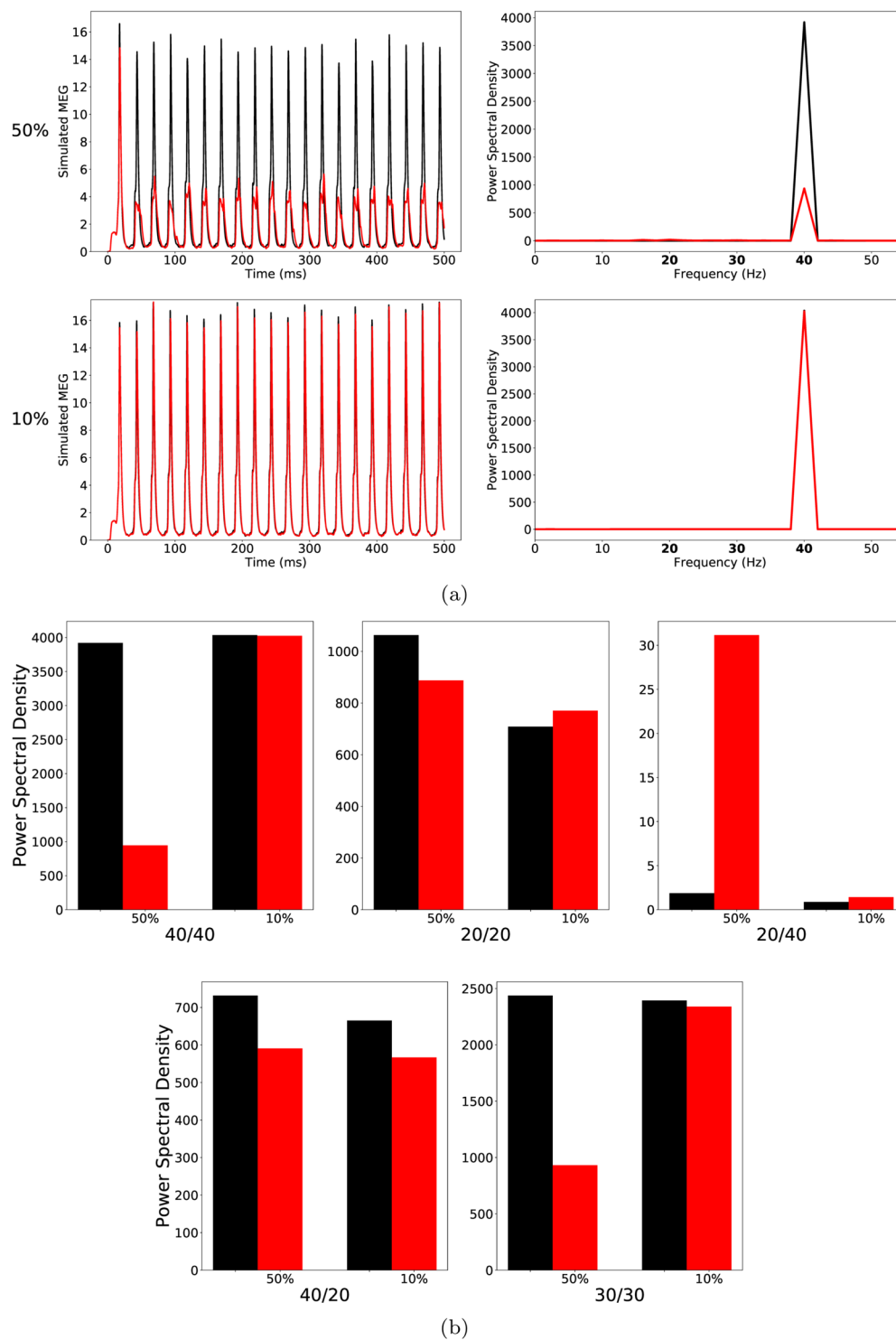


Figure 1. (a) Left row: Raw simulated MEG signals for high (50%) and low (10%) percentage of chandelier cells among total inhibitory cells for a drive frequency of 40 Hz and the two network conditions ('control': black traces; 'schizophrenia-like': red traces). Right row: Power spectral density of the MEG signals of the left row. (b) Comparison of the 5 entrainment measures between control (black) and 'schizophrenia-like' (red) for high and low ChC percentages. Note that 'schizophrenia-like' here means that IPSC decay times at chandelier cell synapses were increased from 8 ms to 28 ms. All traces here depict the mean signal averaged over 20 trials with different realisations of the Poisson process underlying the generation of noise. Importantly, averaging was performed in the time domain prior to a transformation into the frequency domain via Fourier transform, which is also the standard procedure in experiments.

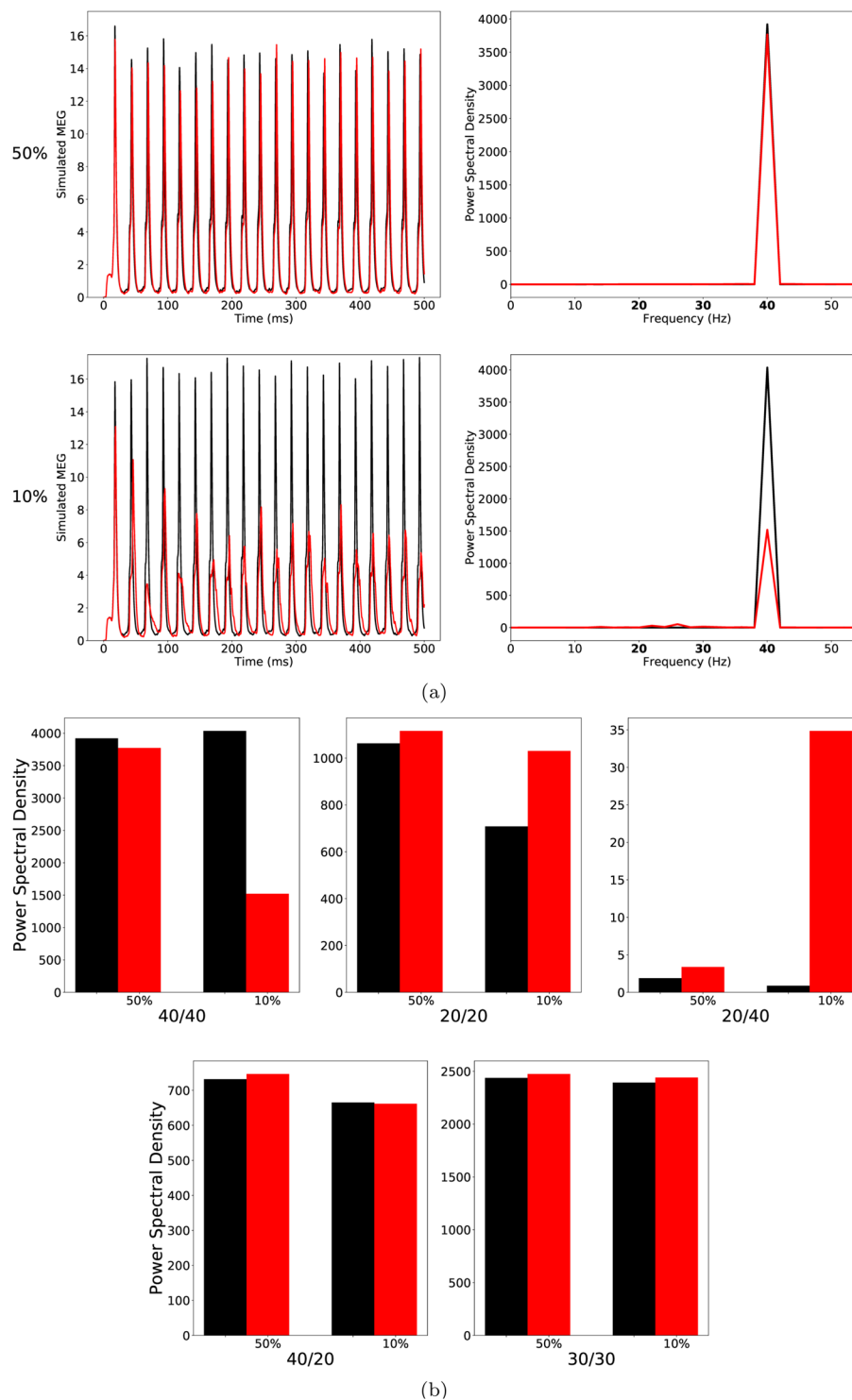


Figure 2. (a) Left row: Raw simulated MEG signals for high (50%) and low (10%) percentage of chandelier cells among total inhibitory cells for a drive frequency of 40 Hz and the two network conditions ('control': black traces; 'schizophrenia-like': red traces). Right row: Power spectral density of the MEG signals of the left row. (b) Comparison of the 5 entrainment measures between control (black) and 'schizophrenia-like' (red) for high and low ChC percentages. Note that 'schizophrenia-like' here means that IPSC decay times at basket cell synapses were increased from 8 ms to 20 ms. All traces here depict the mean signal averaged over 20 trials with different realisations of the Poisson process underlying the generation of noise. Importantly, averaging was performed in the time domain prior to a transformation into the frequency domain via Fourier transform, which is also the standard procedure in experiments.

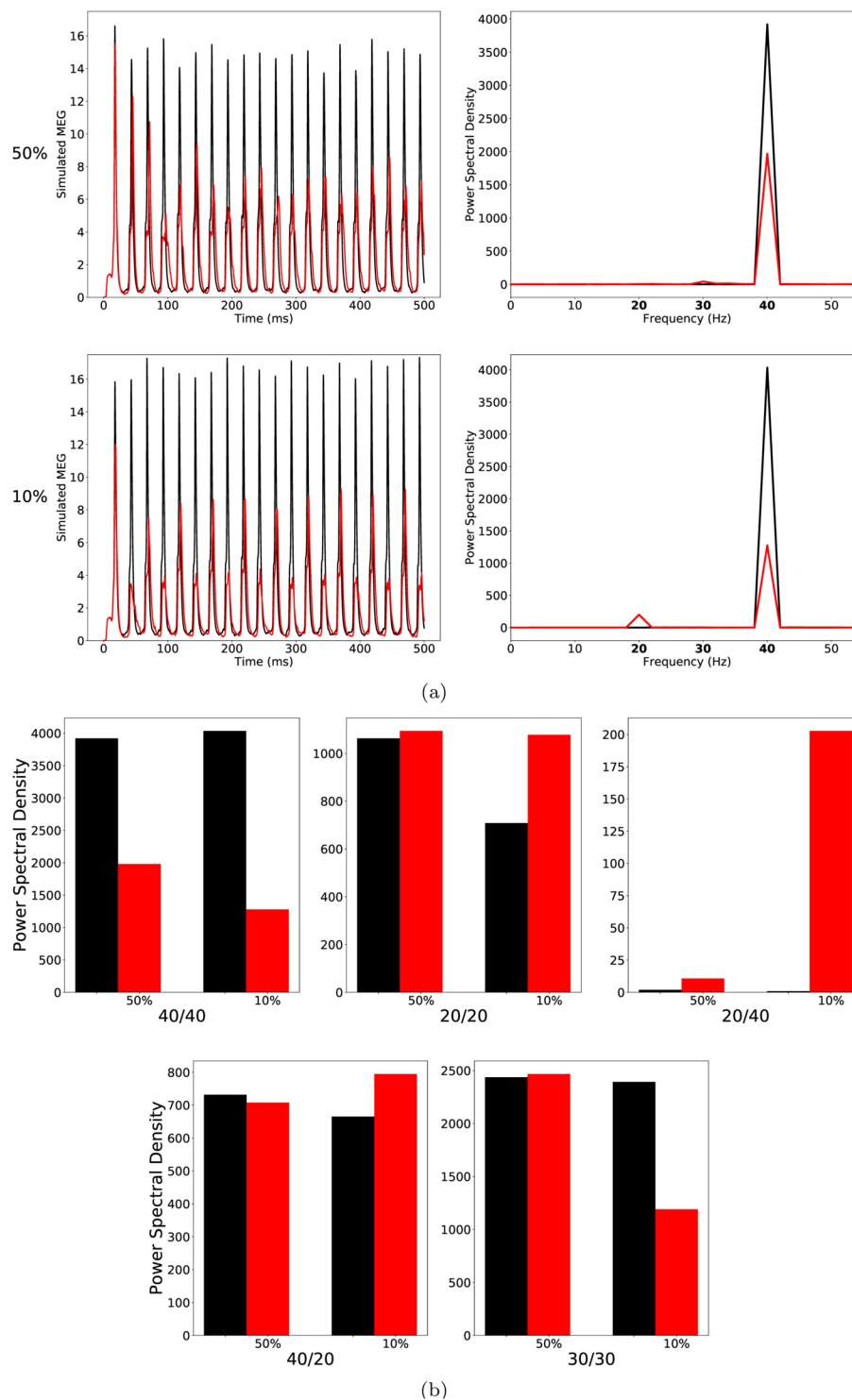


Figure 3. As Fig. 2, but the IPSC decay times at basket cell synapses were increased to 28 ms to model ‘schizophrenia-like’ networks. (a) left row: Raw simulated MEG signals for high (50%) and low (10%) percentage of chandelier cells among total inhibitory cells for a drive frequency of 40 Hz and the two network conditions (‘control’: black traces; ‘schizophrenia-like’: red traces). Right row: Power spectral density of the MEG signals of the left row. (b) Comparison of the 5 entrainment measures between control (black) and ‘schizophrenia-like’ (red) for high and low ChC percentages. All traces here depict the mean signal averaged over 20 trials with different realisations of the Poisson process underlying the generation of noise. Importantly, averaging was performed in the time domain prior to a transformation into the frequency domain via Fourier transform, which is also the standard procedure in experiments.

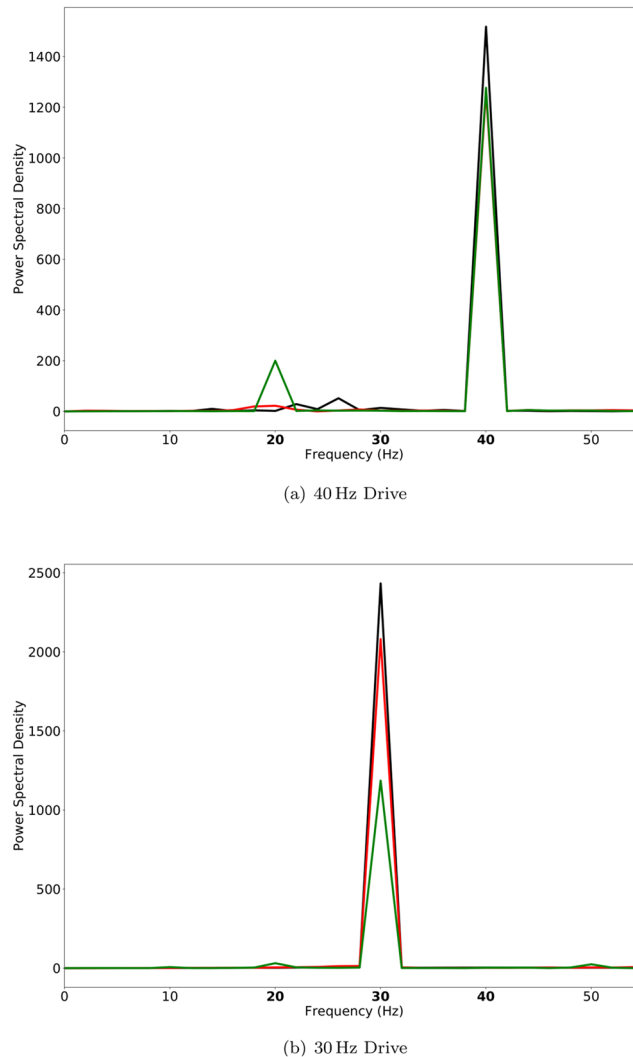


Figure 4. Power spectral density of simulated MEG signals for a ChC percentage of 10% for three different ‘schizophrenia-like’ networks with IPSC decay times at basket cells increased to 20 ms (black), 24 ms (red), and 28 ms (green), respectively. The network receives drive with a frequency of (a) 40 Hz and (b) 30 Hz.

condition, in disagreement with experimental findings^{7,8}. For biologically realistic low ChC percentages we also found a strong reduction of the 40/40 measure (Fig. 5(a)), and a small reduction of the 40/20 measure (Fig. 5(b)). Interestingly, in this case the 20/20 measure was increased and, although still low, the 20/40 measure was also increased, while the 30/30 measure was only marginally different. Overall, the changes in spectral composition were consistent with experimental findings suggesting a general gamma deficit and beta increase in schizophrenia⁸, similar to the case of $\tau_{BC} = 20$ ms.

Lastly, we increased the IPSC times at BC-PC synapses further to 28 ms and, simultaneously, also increased IPSC times at ChC-PC synapses to 40 ms. In the low ChC percentage condition, this further reduced the 40/40 amplitude while increasing the 20/20 measure. Additionally, a 20/40 peak emerged. However, there was also a strong reduction of the 30/30 measure (Fig. 6). Overall, these results here are very similar to the results from the simulations where only IPSC times at BC-PC synapses were modified, suggesting a minor role of ChCs in the generation of ASSR deficits in schizophrenia.

Excitatory effects of chandelier cells. Several *in vitro* studies have demonstrated an excitatory effect of ChC synapses onto PCs, most likely due to differences in the GABAergic reversal potential at the axon initial segment of PCs compared to somatic or dendritic segments. Therefore, we next wondered whether an excitatory effect of ChC-PC neurotransmission together with the increased IPSC decay times at these synapses might explain the experimentally observed changes in gamma and beta range ASSRs. We simulated a newly configured network model, where the ChC-PC synapses had a positive instead of a negative weight factor α (see Methods for details on the synapse models in the network). First, we confirmed that this new configuration qualitatively reproduced the ASSR behaviour of the control network (see Fig. 7(a)). Next, we increased the IPSC decay times at ChC-PC synapses from 8 ms to 28 ms, as before. As can be seen in Fig. 7(b), excitatory ChC-PC coupling together

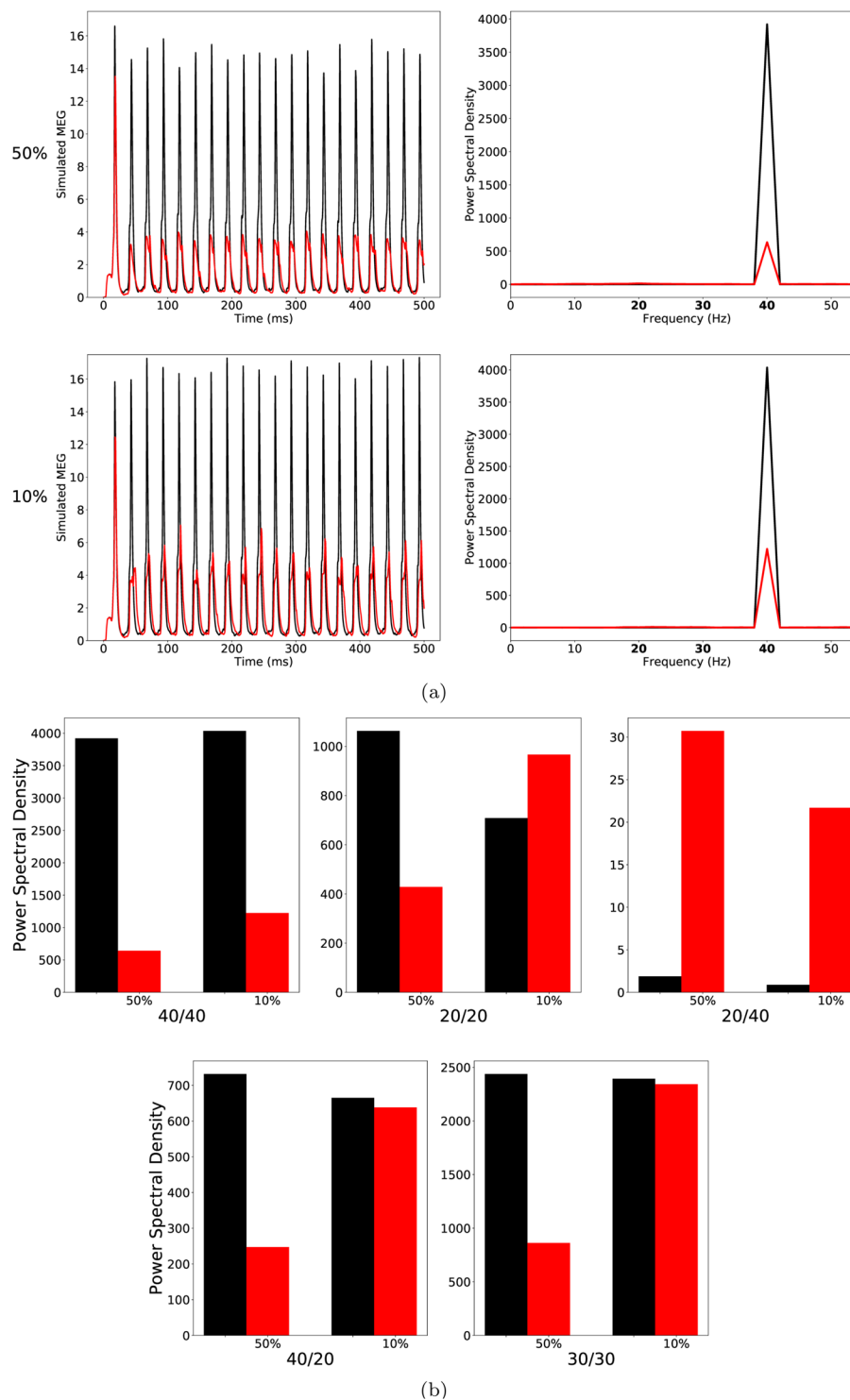


Figure 5. (a) Left row: Raw simulated MEG signals for high (50%) and low (10%) percentage of chandelier cells among total inhibitory cells for a drive frequency of 40 Hz and the two network conditions ('control': black traces; 'schizophrenia-like': red traces). Right row: Power spectral density of the MEG signals of the left row. (b) Comparison of the 5 entrainment measures between control (black) and 'schizophrenia-like' (red) for high and low ChC percentages. Note that 'schizophrenia-like' here means that IPSC decay times at chandelier cell synapses were increased from 8 ms to 28 ms and at basket cell synapses were increased from 8 ms to 20 ms. All traces here depict the mean signal averaged over 20 trials with different realisations of the Poisson process underlying the generation of noise. Importantly, averaging was performed in the time domain prior to a transformation into the frequency domain via Fourier transform, which is also the standard procedure in experiments.

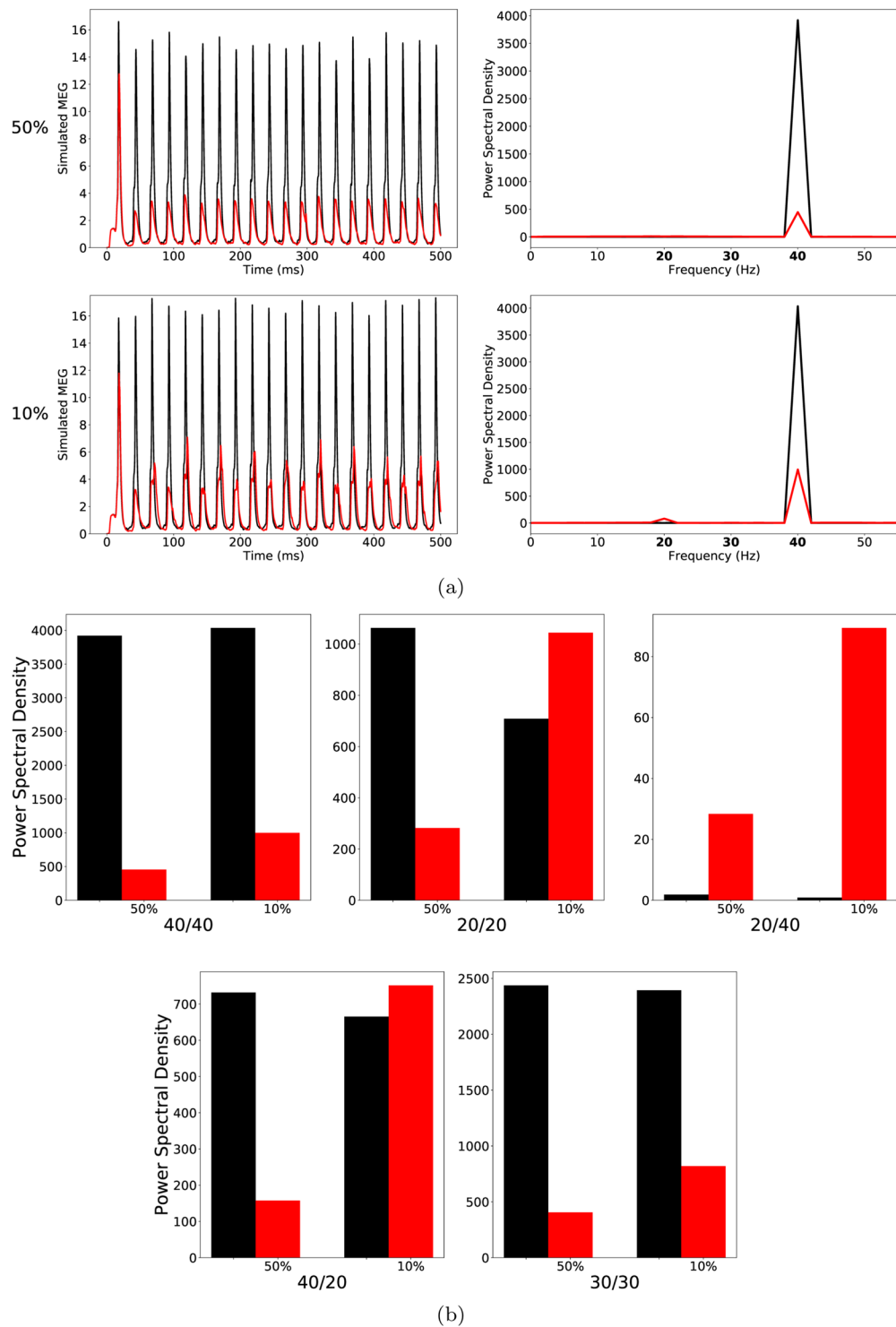


Figure 6. As Fig. 5, but the IPSC decay times at chandelier cell synapses were increased to 40 ms and at basket cell synapses to 28 ms to model ‘schizophrenia-like’ networks. (a) Left row: Raw simulated MEG signals for high (50%) and low (10%) percentage of chandelier cells among total inhibitory cells for a drive frequency of 40 Hz and the two network conditions (‘control’: black traces; ‘schizophrenia-like’: red traces). Right row: Power spectral density of the MEG signals of the left row. (b) Comparison of the 5 entrainment measures between control (black) and ‘schizophrenia-like’ (red) for high and low ChC percentages. All traces here depict the mean signal averaged over 20 trials with different realisations of the Poisson process underlying the generation of noise. Importantly, averaging was performed in the time domain prior to a transformation into the frequency domain via Fourier transform, which is also the standard procedure in experiments.

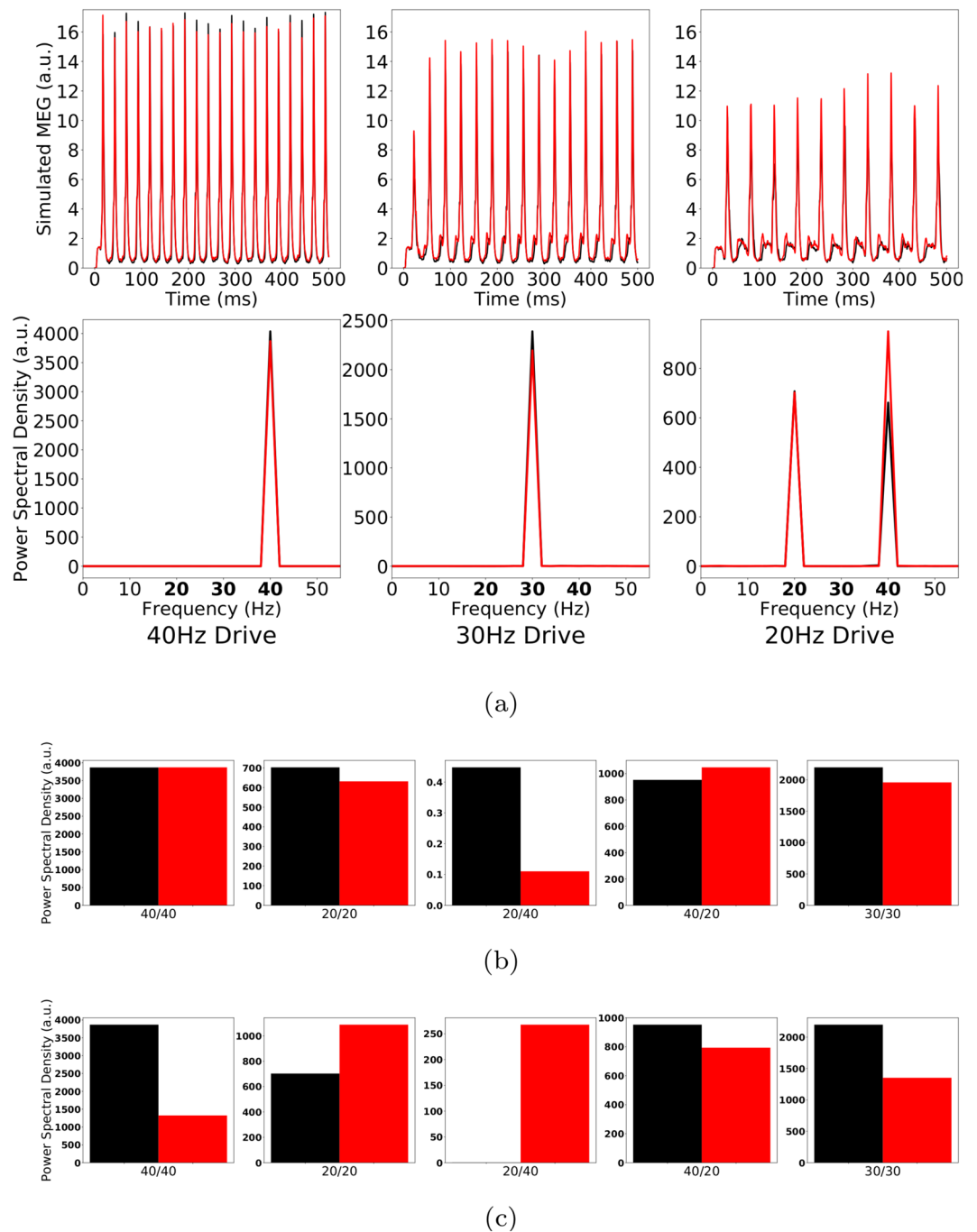


Figure 7. (a) Top row: Simulated MEG signals of a control network with excitatory ChC-PC coupling for a drive of 40, 30 and 20 Hz, respectively. Bottom row: Corresponding power spectral densities. (b) Comparison of the 5 entrainment measures between control (black) and 'schizophrenia-like' (red) in networks with excitatory ChC-PC coupling. Note that 'schizophrenia-like' here means that the IPSC decay time was increased from 8 ms to 28 ms at chandelier cells. (c) Same as (b), however, the IPSC times were increased at basket cells.

with prolonged IPSC times did not lead to substantial changes in any of the 5 entrainment measures. Last, we tested whether excitatory ChC-PC synapses would modulate the ASSR changes caused by prolonged IPSC decay times at BC-PC synapses we had seen before. Therefore, we increased the IPSC decay times at BC-PC synapses from 8 ms to 28 ms in the newly configured network model. Figure 7(c) shows that the excitatory ChC-PC coupling also did not substantially alter the ASSR changes caused by BC-PC synaptic changes.

NMDAR hypofunction. Lastly, we explored the consequences of an NMDAR hypofunction at ChC interneurons by first investigating the effect of NMDAR hypoactivation in isolation and subsequently, together with increased IPSC at ChC-PC and BC-PC synapses, respectively. Since our network does not explicitly model

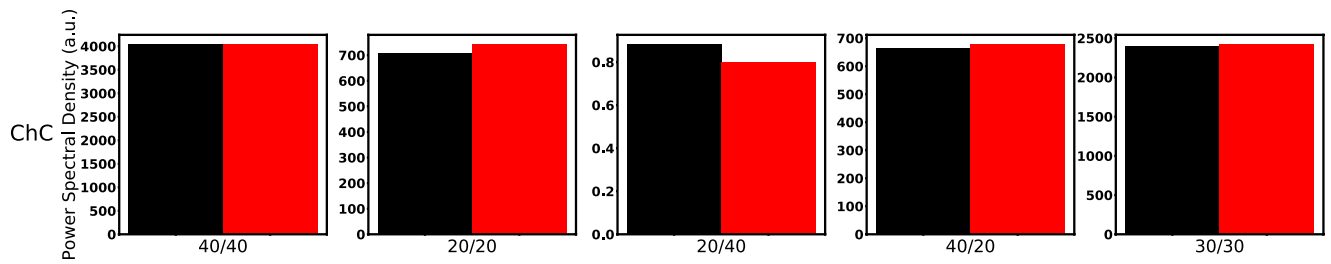
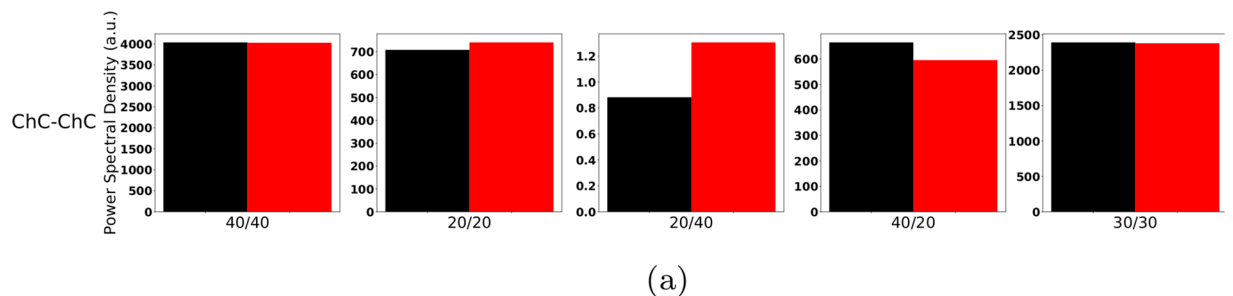
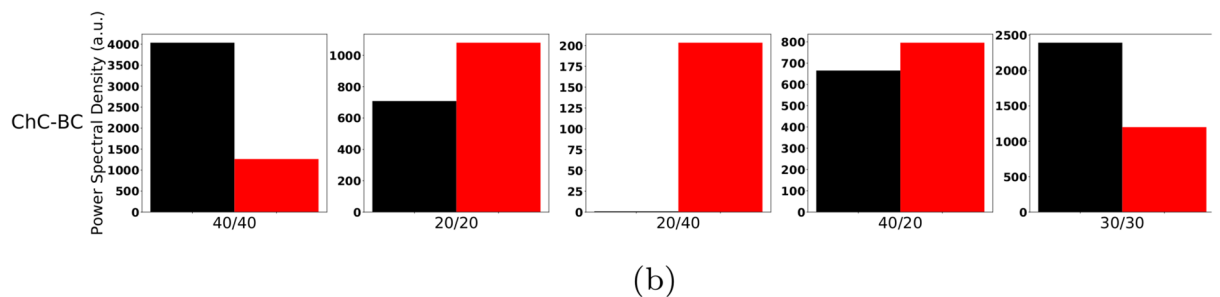


Figure 8. Comparison of the 5 entrainment measures between control (black) and 'schizophrenia-like' (red) for low ChC percentages. Note that 'schizophrenia-like' here means that NMDAR hypofunction was modelled as a strong reduction of excitability of chandelier cells. All traces here depict the mean signal averaged over 20 trials with different realisations of the Poisson process underlying the generation of noise. Importantly, averaging was performed in the time domain prior to a transformation into the frequency domain via Fourier transform, which is also the standard procedure in experiments.



(a)



(b)

Figure 9. Comparison of the 5 entrainment measures between control (black) and 'schizophrenia-like' (red) for low ChC percentages. Note that 'schizophrenia-like' here means that NMDAR hypofunction was modelled as a strong reduction of excitability of chandelier cells and additionally the IPSC decay times at (a) chandelier cell synapses and at (b) basket cell synapses were increased from 8 ms to 28 ms, respectively. All traces here depict the mean signal averaged over 20 trials with different realisations of the Poisson process underlying the generation of noise. Importantly, averaging was performed in the time domain prior to a transformation into the frequency domain via Fourier transform, which is also the standard procedure in experiments.

NMDA receptors, we modelled NMDA hypoactivation as a reduction of ChC excitability (see Methods for implementation details) similar to previous modelling efforts⁴⁵.

We found that NMDAR hypofunction at ChC interneurons did not substantially alter the networks response to the oscillatory drive. Figure 8 shows that none of the 5 entrainment measures showed a large difference between the control and NMDAR hypofunction condition despite the decrease in NMDAR-mediated excitation modelled being relatively large. Furthermore, NMDAR hypofunction at ChCs combined with an increased IPSC decay time did not change the effect increased IPSC times showed in isolation, neither for IPSC increases at ChCs (compare Figs. 9(a) and 1(b)) nor for IPSC changes at BCs (compare Figs. 9(b) and 3(b)).

Discussion

Here, we explored the contribution of slower IPSC dynamics at ChC-PC synapses to gamma and beta range ASSR deficits in patients with schizophrenia using a model cortical network. Generally, at realistic, low ratios of ChCs to BCs, increased IPSC decay times at ChC synapses alone hardly had any influence on ASSRs. At low ChC/BC ratios, increased decay times at BC-PC synapses, on the other hand, strongly altered the spectral composition of ASSRs, replicating several characteristics found experimentally. For a moderate increase (i.e. $\tau_{BC} = 20$ ms), we found a strong decrease of the 40/40 measure, an increase of the 20/20 measure and an increase of the 20/40

measure, although it remained low (Fig. 2). This suggests that this change shifts the preferred frequency of the network from the gamma range more towards the beta range and gives an explanation of the reduced gamma seen across many experiments. Furthermore, the 30/30 measure remained virtually unaffected. However, it did not explain the strong 20/40 component seen by Vierling-Claassen *et al.*⁸. For a stronger increase (i.e. $\tau_{BC} = 28$ ms), we found an even stronger decrease of the 40/40 measure, a further increase of the 20/20 measure and a much stronger increase of the 20/40 measure (see Fig. 3). However, we also saw an increase of the 40/20 measure, contradictory to the gamma to beta shift hypothesis. Furthermore, the 30/30 measure becomes greatly reduced (Fig. 3(b)), which is not seen experimentally. Looking at the power spectra for 40 Hz and 30 Hz drive for increasing τ_{BC} , we see that with longer decay time the 20/40 measure gets stronger but at the same time the change to the network increasingly affects the 30/30 measure (Fig. 4). Lastly, when looking at the effect of increased decay times of ChC-PC synapses in a network where also BC-PC synapse dynamics are slowly decaying, we see that the additional contribution of ChC-mediated effects is very weak for different combinations of decay times τ_{BC} and τ_{ChC} (see Figs. 5 and 6). One interesting effect, however, was the smaller 20/40 measure here compared to the condition where only BC-PC synapses had longer decay times (compare Figs. 3 and 6). Additional to the more classical view that GABAergic chandelier cells provide inhibitory input to pyramidal cells, we have also explored the potential effect of an excitatory ChC-PC coupling, which has been proposed recently^{23–26}. However, at low ChC percentages, we did not see a substantial effect of this excitatory coupling, neither did it change the response to oscillatory drive in the control network, i.e. without alterations of the dynamics of GABAergic synapses, nor did it modulate the effect of changed GABAergic dynamics (see Fig. 7). Since changes to the GABAergic system in schizophrenia have been hypothesized to be a secondary effect due to NMDAR hypofunction at inhibitory interneurons, we also explored the potential contribution of reduced slow NMDA currents at ChC cells. Again, we saw that strongly reduced NMDAR function did hardly affect the ASSRs of the network at low ChC percentages.

Overall, our findings suggest that at realistic, low ratios of ChCs to BCs in a microcircuit, gamma and beta range changes to the spectral composition of ASSRs as seen in SCZ patients, can be well explained by an increase of GABAergic decay times at BC-PC synapses. While postmortem studies indicate that the reduction in GAT1 in SCZ patients preferentially affects ChCs⁴⁶, this might simply reflect easier detection due to the specific morphology of ChC synaptic cartridges compared to BC synapses and not a general difference in GAT1 reduction between the two subtypes. Nevertheless, prolonged IPSC decay times as a result of reduced GAT1 levels requires a high synapse density³¹ and, thus, it is not immediately clear if a GAT1 reduction would be sufficient to cause a prolonged IPSC time course at BC synapses. Interestingly, however, repeated activation together with a reduction in GAT1 also resulted in an increase in IPSC decay times in the study of Overstreet *et al.*³¹. Therefore, increased IPSC times might also be present at BC synapses, especially in a gamma and beta entrainment setting where the network is driven with a relatively high frequency.

Our results demonstrate that prolonged IPSC decay times at BC-PC synapses robustly lead to a weakening of gamma synchronization, especially during gamma drive but also during beta drive. This is consistent with a large body of experimental evidence reporting reduced gamma band power during ASSR paradigms^{7–17} but also during various sensory (e.g. a visual Gestalt task⁵), and cognitive tasks (e.g. a working memory task⁴⁷). We also found an increase of beta synchronization during beta drive, and, although in most conditions still very small, increased beta synchronization during gamma drive. This reproduces the findings of Vierling-Claassen *et al.*⁸ that slow dynamics at FS PV⁺ interneurons might not only desynchronize gamma oscillations but also shift the preferred frequency of cortical networks from gamma to the beta band. However, our results further demonstrate that, most likely, BCs are the main interneuron subtype causing this shift and not ChCs, as hypothesized by Vierling-Claassen *et al.*⁸. Furthermore, we found that while longer decay times at BC-PC synapses led to a stronger and more robust peak of the 20/40 measure, they also introduced a stronger reduction of the 30/30 measure. Given that studies have consistently reported that the 30/30 measure remains unaffected in SCZ patients^{7,8,17}, together with the fact that the strong 20/40 component has not been reported by experimental studies except for Vierling-Claassen *et al.*⁸, our results suggest that a strong 20/40 component might not be a core ASSR deficit in patients with schizophrenia. This is further underpinned by the finding that alterations at ChCs together with BC alterations, led to a reduction of the 20/40 measure compared to the condition where only BC-PC had prolonged decay times.

While the results presented here suggest a modulatory influence of ChC alterations on gamma and beta oscillations at most, we have to note that the employed model has substantial limitations. Our model, for example, does not explore the possibility that, due to the location directly at the axon initial segment, ChCs might exert significantly stronger control over PC firing, which in turn might counterbalance their small numbers. While we have investigated the potential consequences of NMDAR hypofunction affecting ChCs, we haven't explored NMDAR hypofunction in BCs because we were primarily interested to understand the contribution of ChCs within this model of prolonged IPSC times. Experimental and computational studies have linked NMDAR hypofunction to gamma deficits^{48,49} and further research in this area is definitely warranted. However, we must admit that our model is not very well suited for this task because NMDARs are not explicitly modelled. Finally, the theta neuron model is a simple and abstract neuron model and does not capture electrophysiological differences between BCs and ChCs found experimentally²². Interestingly, genetic variants of risk genes for schizophrenia include a variety of genes coding for ion channels or ion transporters, which have been shown to alter cell excitability^{50,51} and network oscillations⁵². Such variants might potentially amplify electrophysiological differences between BCs and ChCs and thereby change their relative roles in the generation of gamma/beta oscillations.

In summary, our findings suggest that ChCs are likely not strongly involved in gamma/beta range ASSR deficits in schizophrenia, and, therefore future modelling efforts should focus on alterations at BC-PC synapses. Furthermore, ChC-PC synapses might not represent a valuable target for therapeutic interventions aiming at restoring the gamma ASSR in patients with schizophrenia.

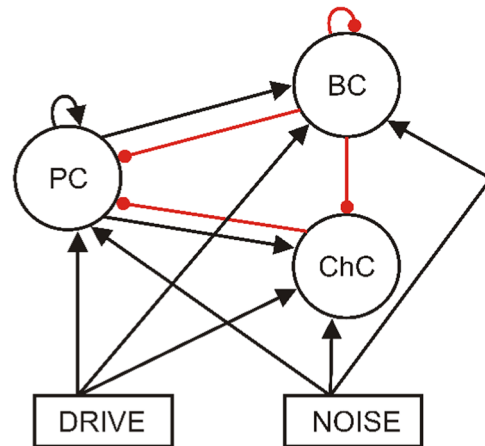


Figure 10. Schematic representation of the network structure. All three populations receive drive and noise input. The excitatory population makes connections to itself and to both inhibitory populations. Similarly, the basket cell population inhibits itself and both other populations. The chandelier cell population, however, exclusively targets the excitatory cells. (Black arrow: excitatory connection. Red arrow: inhibitory connection.)

Methods

The model. The model proposed here is based on a recent reimplementation⁵³ of the simple model presented by Vierling-Claassen *et al.*⁸. However, we extended the model to consist of two distinct inhibitory populations (instead of only one), one representing basket cells and one representing chandelier cells (see Fig. 10).

Single cell model. Individual cells are modeled as theta neurons (for a detailed discussion of this neuron model see e.g. Boegers *et al.*⁵⁴).

The k th neuron in a network is described by a single variable θ_k , which can be regarded as the neuron state, subject to the following dynamics

$$\frac{d\theta_k}{dt} = 1 - \cos\theta_k + (b + S_k + N(t)) \cdot (1 + \cos\theta_k)$$

where b is an externally applied current, S is the total synaptic input to the cell and $N(t)$ is a time-varying noise input. Total synaptic input to a cell in a network is calculated as

$$S_k = \sum_{j=1}^n \alpha_j \cdot g_{jk} \cdot s_{jk}$$

where n is the number of presynaptic neurons, α_j controls excitation and inhibition, i.e. is +1 for excitatory synapses and -1 for inhibitory ones, g_{jk} is the synaptic strength from cell j to cell k and s_{jk} is the synaptic gating variable from cell j to cell k . Synaptic gating variables are subject to the following dynamics

$$\frac{ds_{jk}}{dt} = -\frac{s_{jk}}{\tau_j} + e^{-\eta \cdot (1 + \cos\theta_j)} \cdot \frac{1 - s_{jk}}{\tau_R}$$

where τ_j is the synaptic decay time, τ_R the synaptic rise time and η is a scaling parameter. The network receives excitatory drive input at click train frequency from a single pacemaker cell. Additionally, Poissonian noise input is also given to all cells in the network. A noise spike at time t_n elicits the following excitatory postsynaptic potential ('EPSP')

$$N = H(t - t_n) \cdot \frac{A \cdot g_{gmax} \cdot (e^{-(t-t_n)/\tau_{exc}} - e^{-(t-t_n)/\tau_R})}{\tau_{exc} - \tau_R}$$

where $A \cdot g_{gmax}$ is the strength of the noise, τ_{exc} is the synaptic decay time, τ_R the synaptic rise time, and H the Heaviside function. An overview of all the model parameters used in this study can be found in Table 2.

Network. We combined 80 excitatory, pyramidal cells together with 40 inhibitory cells of the two different inhibitory subtypes (basket and chandelier cells) into a network model, following the earlier work of Vierling-Claassen *et al.*⁸. The percentages of the two different subtypes varied.

The connectivity of the network is summarized in Fig. 10. Pyramidal cells make connections to other pyramidal cells, as well as to both types of inhibitory interneurons. Basket cells inhibit pyramidal cells, themselves and chandelier cells. Chandelier cells only inhibit pyramidal cells (see e.g. Tremblay *et al.*²¹). The connectivity between

Parameter	Definition	Value
n_E	Exc. population size	80
n_I	Inh. population size (BCs and ChCs together)	40
	<i>Note that percentages of the two different types varies</i>	
τ_R	Synaptic rise time	0.1
τ_{exc}	Excitatory decay time	2.0
τ_{bc}	BC decay time	8.0
τ_{chc}	ChC decay time	8.0
g_{ee}	E-E synaptic strength	0.00375
g_{ebc}	E-BC synaptic strength	0.00625
g_{echc}	E-ChC synaptic strength	0.00625
g_{bce}	BC-E synaptic strength	0.00375
g_{che}	ChC-E synaptic strength	0.00375
g_{bcb}	BC-BC synaptic strength	0.005
g_{de}	Synaptic strength of drive to E cells	0.3
g_{dbc}	Synaptic strength of drive to BC cells	0.08
g_{dchc}	Synaptic strength of drive to ChC cells	0.08
b	Applied current (regardless of cell type)	-0.1
Ag_{max}	Scaling factor for noise EPSCs	0.6

Table 2. Model parameters.

any two populations is all-to-all. All populations also have two sources of input, the oscillatory drive input and a background noise input. The drive input periodically sends spikes with a given frequency to all three populations. In order to generate the spikes a drive cell is implemented (also a theta neuron), which receives an applied current so that its spike frequency matches the driving frequency. This drive cell is then connected to all cells in the network. The background noise input sends noise spikes at times drawn from a Poisson distribution.

Entrainment measures. In order to evaluate the oscillatory entrainment we record the spiking of the three populations as well as a simulated ‘EEG/MEG’ signal, calculated as the sum of all excitatory synaptic variables over all pyramidal cells⁸. As the main measure for entrainment we perform an FFT on the ‘EEG/MEG’ signal and extract the power in certain frequency bands. Since we are mainly interested in entrainment in the gamma and beta band, we specifically look at five measures (see experimental studies^{7,8}): 1) 40 Hz power at 40 Hz drive 2) 20 Hz power at 40 Hz drive 3) 20 Hz power at 20 Hz drive 4) 40 Hz power at 20 Hz drive 5) 30 Hz power at 30 Hz drive (which will hereafter be referred to as the **40/40 measure**, the **20/40 measure**, the **20/20 measure**, the **40/20 measure** and the **30/30 measure**, respectively). As can be seen in Table 1, a decrease in the 40/40 measure is a robust finding in all three considered studies. Furthermore, the 30/30 measure is not affected in all three studies. Beyond the 40/40 measure, only the study by Vierling-Claassen *et al.*⁸ found significant differences for other measures, namely, a decrease in the 40/20 measure, underpinning the deficit in gamma generation, and an increase in the 20/20 and the 20/40 measures, suggesting a transfer of power from the gamma to the beta band in patients with schizophrenia. It is important to note here, that both the Kwon *et al.*⁷ and the Krishnan *et al.*⁹ studies, used EEG whereas the Vierling-Claassen *et al.*⁸ study used MEG and that it has been argued that MEG might have a higher sensitivity, which could explain the absence of findings other than for the 40/40 measure in the first two studies. Overall, given the experimental evidence discussed above, we think that the five measures chosen provide a good coverage of the frequency bands that are important to understand gamma and beta entrainment deficits in schizophrenia.

Implementation. The model was implemented using Python 2.7.9 and numpy 1.9.3. Analysis and visualization of the model output was also done in Python using the numpy and matplotlib packages (matplotlib 1.4.3).

All differential equations were solved using a simple forward Euler scheme. A single simulation simulated a 500 ms trial and the time step was chosen such that this results in $2^{13} = 8192$ data points. However, the main results were unaffected by using a smaller time step.

All code (for simulations, analysis and visualization) has been made publicly available in the following github repository: <https://github.com/ChristophMetzner/Chandelier-Basket-Model>.

Exploration of circuit abnormalities. We explored the effects of natural differences between BCs and ChCs together with their differential schizophrenia-associated abnormalities on oscillatory entrainment in the gamma and beta frequency range. Specifically, we investigated the ratio of BCs versus ChCs, a prolonged IPSC decay times of inhibitory synapses of both interneuron subtypes (because of a reduced expression of GAT1 for both BCs and ChCs and an increased expression of α_2 subunits for ChCs), the putative excitatory effect of ChC-PC synapses and reduced levels of ChC excitability due to NMDAR hypoactivation. Table 3 details how these changes were modelled.

Experimental finding	Parameter change in the model
BC/ChC ratio	$[n_{BC}, n_{ChC}]$: [20, 20], [30, 10], [36, 4], [38, 2]
Increased IPSC decay time at BC synapses	τ_{BC} : 20 ms, 24 ms, 28 ms (instead of 8 ms)
Increased IPSC decay time at ChC synapses	τ_{ChC} : 28 ms, 35 ms, 40 ms (instead of 8 ms)
Excitatory ChC-PC synapses	α_j for ChC-PC synapses: +1 (instead of -1)
NMDAR hypoactivation	b_{ChC} : -0.05 (instead of -0.01)

Table 3. Modelling of interneuron differences and circuit abnormalities.

Because of the Poissonian background noise input, simulation results varied from trial to trial. To capture the robustness of findings we always performed 20 simulation trials, each with a different realisation of the underlying Poissonian noise process. When analysing the effect of circuit abnormalities, we averaged the 20 trials for each condition in time to get an average simulated MEG signal and calculated a power spectral density of this signal.

Received: 21 June 2019; Accepted: 12 October 2019;

Published online: 06 December 2019

References

- Fries, P. A mechanism for cognitive dynamics: neuronal communication through neuronal coherence. *Trends in cognitive sciences* **9**, 474–480 (2005).
- Fries, P. Rhythms for Cognition: Communication through Coherence, <https://doi.org/10.1016/j.neuron.2015.09.034>, 15334406 (2015).
- Salinas, E. & Sejnowski, T. J. Correlated neuronal activity and the flow of neural information. *Nature reviews. Neuroscience* **2**, 539 (2001).
- Howard, M. W. *et al.* Gamma oscillations correlate with working memory load in humans. *Cerebral cortex* **13**, 1369–1374 (2003).
- Spencer, K. M. *et al.* Abnormal neural synchrony in schizophrenia. *The Journal of Neuroscience* **23**, 7407–7411 (2003).
- Cho, R. Y., Konecky, R. O. & Carter, C. S. Impairments in frontal cortical gamma synchrony and cognitive control in schizophrenia. *Proceedings of the National Academy of Sciences* **103**, 19878–19883 (2006).
- Kwon, J. S. *et al.* Gamma frequency–range abnormalities to auditory stimulation in schizophrenia. *Archives of General Psychiatry* **56**, 1001–1005 (1999).
- Vierling-Claassen, D., Siekmeier, P., Stufflebeam, S. & Kopell, N. Modeling GABA alterations in schizophrenia: a link between impaired inhibition and altered gamma and beta range auditory entrainment. *Journal of Neurophysiology* **99**, 2656–2671 (2008).
- Krishnan, G. P. *et al.* Steady state and induced auditory gamma deficits in schizophrenia. *Neuroimage* **47**, 1711–1719 (2009).
- Teale, P. *et al.* Cortical source estimates of gamma band amplitude and phase are different in schizophrenia. *Neuroimage* **42**, 1481–1489 (2008).
- Tsuhimoto, R. *et al.* Reduced high and low frequency gamma synchronization in patients with chronic schizophrenia. *Schizophrenia research* **133**, 99–105 (2011).
- Light, G. A. *et al.* Gamma band oscillations reveal neural network cortical coherence dysfunction in schizophrenia patients. *Biological psychiatry* **60**, 1231–1240 (2006).
- Brenner, C. A., Sporns, O., Lysaker, P. H. & O'Donnell, B. F. EEG synchronization to modulated auditory tones in schizophrenia, schizoaffective disorder, and schizotypal personality disorder. *American Journal of Psychiatry* **160**, 2238–2240 (2003).
- Spencer, K. M., Salisbury, D. F., Shenton, M. E. & McCarley, R. W. Gamma-Band auditory steady-state responses are impaired in first episode psychosis. *Biological psychiatry* **64**, 369–375 (2008).
- Spencer, K. M. The functional consequences of cortical circuit abnormalities on gamma oscillations in schizophrenia: insights from computational modeling. *Frontiers in Human Neuroscience* **3** (2009).
- Spencer, K. M. Baseline gamma power during auditory steady-state stimulation in schizophrenia. *Frontiers in Human Neuroscience* **5**, 190, <https://doi.org/10.3389/fnhum.2011.00190> (2012).
- Thuné, H., Recasens, M. & Uhlhaas, P. J. The 40-Hz auditory steady-state response in patients with schizophrenia a meta-Analysis. *JAMA Psychiatry*, <https://doi.org/10.1001/jamapsychiatry.2016.2619> (2016).
- Hajos, N. Spike Timing of Distinct Types of GABAergic Interneuron during Hippocampal Gamma Oscillations *In Vitro*. *Journal of Neuroscience* **24**, 9127–9137, <https://doi.org/10.1523/JNEUROSCI.2113-04.2004> (2004).
- Bartos, M., Vida, I. & Jonas, P. Synaptic mechanisms of synchronized gamma oscillations in inhibitory interneuron networks. *Nature Reviews Neuroscience* **8**, 45–56 (2007).
- Kawaguchi, Y. & Kubota, Y. GABAergic cell subtypes and their synaptic connections in rat frontal cortex. *Cerebral Cortex*, <https://doi.org/10.1093/cercor/7.6.476> (1997).
- Tremblay, R., Lee, S. & Rudy, B. GABAergic Interneurons in the Neocortex: From Cellular Properties to Circuits, <https://doi.org/10.1016/j.neuron.2016.06.033> (2016).
- Povysheva, N. V., Zaitsev, A. V., Gonzalez-Burgos, G. & Lewis, D. A. Electrophysiological Heterogeneity of Fast-Spiking Interneurons: Chandelier versus Basket Cells. *PLoS One* **8**, <https://doi.org/10.1371/journal.pone.0070553> (2013).
- Szabadics, J. *et al.* Excitatory effect of GABAergic axo-axonic cells in cortical microcircuits. *Science*, <https://doi.org/10.1126/science.1121325> (2006).
- Woodruff, A., Xu, Q., Anderson, S. A. & Yuste, R. Depolarizing effect of neocortical chandelier neurons. *Frontiers in neural circuits* **3** (2009).
- Woodruff, A. R., Anderson, S. A. & Yuste, R. The enigmatic function of chandelier cells. *Frontiers in neuroscience* **4** (2010).
- Woodruff, A. R. *et al.* State-dependent function of neocortical chandelier cells. *The Journal of Neuroscience* **31**, 17872–17886 (2011).
- Woo, T.-U., Miller, J. L. & Lewis, D. A. Schizophrenia and the parvalbumin-containing class of cortical local circuit neurons. *American Journal of Psychiatry* **154**, 1013–1015 (1997).
- Beasley, C. L., Zhang, Z. J., Patten, I. & Reynolds, G. P. Selective deficits in prefrontal cortical GABAergic neurons in schizophrenia defined by the presence of calcium-binding proteins. *Biological psychiatry* **52**, 708–715 (2002).
- Hashimoto, T. *et al.* Gene expression deficits in a subclass of GABA neurons in the prefrontal cortex of subjects with schizophrenia. *The Journal of neuroscience: the official journal of the Society for Neuroscience* **23**, 6315–6326, <https://doi.org/10.2967/jnumed.108.060368> (2003).
- Gonzalez-Burgos, G. & Lewis, D. A. GABA neurons and the mechanisms of network oscillations: implications for understanding cortical dysfunction in schizophrenia. *Schizophrenia Bulletin* **34**, 944–961 (2008).

31. Overstreet, L. S. & Westbrook, G. L. Synapse density regulates independence at unitary inhibitory synapses. *Journal of Neuroscience* **23**, 2618–2626 (2003).
32. Keros, S. & Hablitz, J. J. Subtype-specific GABA transporter antagonists synergistically modulate phasic and tonic GABA A conductances in rat neocortex. *Journal of neurophysiology* **94**, 2073–2085 (2005).
33. Volk, D. W., Austin, M. C., Pierri, J. N., Sampson, A. R. & Lewis, D. A. Decreased Glutamic Acid Decarboxylase67 Messenger RNA Expression in a Subset of Prefrontal Cortical γ -Aminobutyric Acid Neurons in Subjects With Schizophrenia. *Archives of General Psychiatry*, <https://doi.org/10.1001/archpsyc.57.3.237> (2000).
34. Lavoie, A., Tingey, J., Harrison, N., Pritchett, D. & Twyman, R. Activation and deactivation rates of recombinant GABA(A) receptor channels are dependent on alpha-subunit isoform. *Biophysical Journal*, [https://doi.org/10.1016/S0006-3495\(97\)78280-8](https://doi.org/10.1016/S0006-3495(97)78280-8) (1997).
35. Javitt, D. C. & Zukin, S. R. Recent advances in the phencyclidine model of schizophrenia. *American Journal of Psychiatry*, <https://doi.org/10.1176/ajp.148.10.1301> (1991).
36. Kristiansen, L. V., Huerta, I., Beneyto, M. & Meador-Woodruff, J. H. NMDA receptors and schizophrenia, <https://doi.org/10.1016/j.coph.2006.08.013> (2007).
37. Kantrowitz, J. T. & Javitt, D. C. N-methyl-d-aspartate (NMDA) receptor dysfunction or dysregulation: The final common pathway on the road to schizophrenia? *Brain Research Bulletin*, <https://doi.org/10.1016/j.brainresbull.2010.04.006>, NIHMS150003 (2010).
38. Beneyto, M. & Meador-Woodruff, J. H. Lamina-specific abnormalities of NMDA receptor-associated postsynaptic protein transcripts in the prefrontal cortex in schizophrenia and bipolar disorder. *Neuropsychopharmacology*, <https://doi.org/10.1038/sj.npp.1301604> (2008).
39. Hahn, C.-G. *et al.* Altered neuregulin 1–erbB4 signaling contributes to NMDA receptor hypofunction in schizophrenia. *Nature medicine* **12**, 824–828 (2006).
40. Stelllet, P., Neijt, H. C., Cuenod, M. & Do, K. Q. Synaptic plasticity impairment and hypofunction of NMDA receptors induced by glutathione deficit: relevance to schizophrenia. *Neuroscience* **137**, 807–819 (2006).
41. Wonodi, I. *et al.* Downregulated kynurenine 3-monooxygenase gene expression and enzyme activity in schizophrenia and genetic association with schizophrenia endophenotypes. *Archives of general psychiatry* **68**, 665–674 (2011).
42. Vierling-Claassen, D. & Kopell, N. The dynamics of a periodically forced cortical microcircuit, with an application to schizophrenia. *SIAM Journal on Applied Dynamical Systems* **8**, 710–733 (2009).
43. Markram, H. *et al.* Interneurons of the neocortical inhibitory system, <https://doi.org/10.1038/nrn1519>, NIHMS150003 (2004).
44. Defelipe, J., Hendryt, S. H. C. & Jonest, E. G. Visualization of chandelier cell axons by parvalbumin immunoreactivity in monkey cerebral cortex (interneurons/inhibition). *Tech. Rep.* (1989).
45. Carlén, M. *et al.* A critical role for NMDA receptors in parvalbumin interneurons for gamma rhythm induction and behavior. *Mol. Psychiatry* **17**, 537–548, <https://doi.org/10.1038/mp.2011.31> (2012).
46. Lewis, D. A., Hashimoto, T. & Volk, D. W. Cortical inhibitory neurons and schizophrenia, <https://doi.org/10.1038/nrn1648> (2005).
47. Chen, C. M. A. *et al.* GABA level, gamma oscillation, and working memory performance in schizophrenia. *NeuroImage: Clinical*, <https://doi.org/10.1016/j.nicl.2014.03.007> (2014).
48. Kirli, K. K., Ermentrout, G. B. & Cho, R. Y. Computational study of NMDA conductance and cortical oscillations in schizophrenia. *Frontiers in computational neuroscience* **8** (2014).
49. Jadi, M. P., Behrens, M. M. & Sejnowski, T. J. Abnormal Gamma Oscillations in N-Methyl-D-Aspartate Receptor Hypofunction Models of Schizophrenia, <https://doi.org/10.1016/j.biopsych.2015.07.005> (2016).
50. Mäki-Marttunen, T. *et al.* Functional effects of schizophrenia-linked genetic variants on intrinsic single-neuron excitability: A modeling study. *Biological Psychiatry: Cognitive Neuroscience and Neuroimaging* **1**, 49–59 (2016).
51. Mäki-Marttunen, T. *et al.* Pleiotropic effects of schizophrenia-associated genetic variants in neuron firing and cardiac pacemaking revealed by computational modeling. *Translational Psychiatry*, <https://doi.org/10.1038/s41398-017-0007-4> (2017).
52. Mäki-Marttunen, T. *et al.* Alterations in Schizophrenia-Associated Genes Can Lead to Increased Power in Delta Oscillations. *Cerebral Cortex*, <https://doi.org/10.1093/cercor/bhy291> (2018).
53. Metzner, C. [Re] Modeling GABA Alterations in Schizophrenia: A Link Between Impaired Inhibition and Gamma and Beta Auditory Entrainment. *ReScience* **3** (2017).
54. Börgers, C. & Kopell, N. Synchronization in networks of excitatory and inhibitory neurons with sparse, random connectivity. *Neural computation* **15**, 509–538 (2003).

Author contributions

C.M., B.Z. and V.S. conceived the study, C.M. implemented the model and ran all the simulations, C.M. analysed the results. All authors discussed the findings and reviewed the manuscript.

Competing interests

The authors declare no competing interests.

Additional information

Correspondence and requests for materials should be addressed to C.M.

Reprints and permissions information is available at www.nature.com/reprints.

Publisher's note Springer Nature remains neutral with regard to jurisdictional claims in published maps and institutional affiliations.



Open Access This article is licensed under a Creative Commons Attribution 4.0 International License, which permits use, sharing, adaptation, distribution and reproduction in any medium or format, as long as you give appropriate credit to the original author(s) and the source, provide a link to the Creative Commons license, and indicate if changes were made. The images or other third party material in this article are included in the article's Creative Commons license, unless indicated otherwise in a credit line to the material. If material is not included in the article's Creative Commons license and your intended use is not permitted by statutory regulation or exceeds the permitted use, you will need to obtain permission directly from the copyright holder. To view a copy of this license, visit <http://creativecommons.org/licenses/by/4.0/>.

© The Author(s) 2019